

Robust Reflectance Estimation for Projection-Based Appearance Control in a Dynamic Light Environment

Ryo Akiyama¹, Student Member, IEEE, Goshiro Yamamoto², Member, IEEE,
Toshiyuki Amano³, Member, IEEE, Takafumi Taketomi⁴, Member, IEEE,
Alexander Plopski⁵, Member, IEEE, Christian Sandor, Member, IEEE,
and Hirokazu Kato⁶, Member, IEEE

Abstract—We present a novel method that robustly estimates the reflectance, even in an environment with dynamically changing light. To control the appearance of an object by using a projector–camera system, an appropriate estimate of the object’s reflectance is vital to the creation of an appropriate projection image. Most conventional estimation methods assume static light conditions; however, in practice, the appearance is affected by both the reflectance and environmental light. In an environment with dynamically changing light, conventional reflectance estimation methods require calibration every time the conditions change. In contrast, our method requires no additional calibration because it simultaneously estimates both the reflectance and environmental light. Our method is based on the concept of creating two different light conditions by switching the projection at a rate higher than that perceived by the human eye and captures the images of a target object separately under each condition. The reflectance and environmental light are then simultaneously estimated by using the pair of images acquired under these two conditions. We implemented a projector–camera system that switches the projection on and off at 120 Hz. Experiments confirm the robustness of our method when changing the environmental light. Further, our method can robustly estimate the reflectance under practical indoor lighting conditions.

Index Terms—Appearance manipulation, environmental light, projector–camera system, reflectance estimation, spatial augmented reality

1 INTRODUCTION

COLORS and textures are essential elements constituting the appearance of objects. Recently, projection mapping technologies have advanced to a point where projectors can control the colors and textures observed on the surfaces of physical objects. They are used for entertainment in amusement parks [1], museum events [2], gaming [3], [4], and educational [5], and medical applications [6].

Many studies have addressed projector–camera systems that are capable of interactively controlling a projection with the changes in the object onto which an image is being projected. For example, there are projection technologies that can project light onto a static object with a complex geometry [7], a face [8], and other deformable objects [9], [10]. Some of these interactive systems first capture the

original colors and textures of the target objects and then artificially change their appearance by overlaying a projection. In the present study, we focus on an interactive projection system with a color-replacing function that we refer to as *Appearance Control* [11]. The system changes an object’s appearance by considering its original reflectance properties. Even when the object moves or new objects appear, the system creates projection images for appearance control by estimating the reflectance of the target object(s). However, the system does not consider dynamically changing environmental light. When the environmental light changes, the system cannot correctly estimate the reflectance unless photometric calibration is performed again.

Although it is possible to recalibrate the system whenever the environmental light changes, this is an impractical approach because the environmental light changes frequently. For example, environmental light continuously changes when there is a window, even indoors. There are also various types of light equipment that can control the color and illuminance. Moreover, it is almost impossible to create a portable appearance control system with current algorithms. In addition, this calibration is carried out by capturing images of red, green, and blue projections on a white plane. Clearly, it would be impractical to repeatedly prepare a white plane for calibration throughout the day. Therefore, appearance control can never be completely practical unless it can be applied under dynamically changing lighting conditions.

- R. Akiyama, T. Taketomi, A. Plopski, and H. Kato are with the Nara Institute of Science and Technology, Ikoma, Nara 630-0192, Japan. E-mail: {akiyama.ryo.ah7, takafumi-t, plopski, kato}@is.naist.jp.
- G. Yamamoto is with the Kyoto University, Kyoto 606-8501, Japan. E-mail: goshiro@kuhp.kyoto-u.ac.jp.
- T. Amano is with the Wakayama University, Wakayama 640-8510, Japan. E-mail: amano@sys.wakayama-u.ac.jp.
- C. Sandor is with the City University of Hong Kong, Kowloon Tong, Hong Kong. E-mail: christian@sandor.com.

Manuscript received 17 Oct. 2018; revised 16 June 2019; accepted 7 Aug. 2019. Date of publication 10 Sept. 2019; date of current version 28 Jan. 2021. (Corresponding author: Ryo Akiyama.)

Recommended for acceptance by D. Schmalstieg.

Digital Object Identifier no. 10.1109/TVCG.2019.2940453

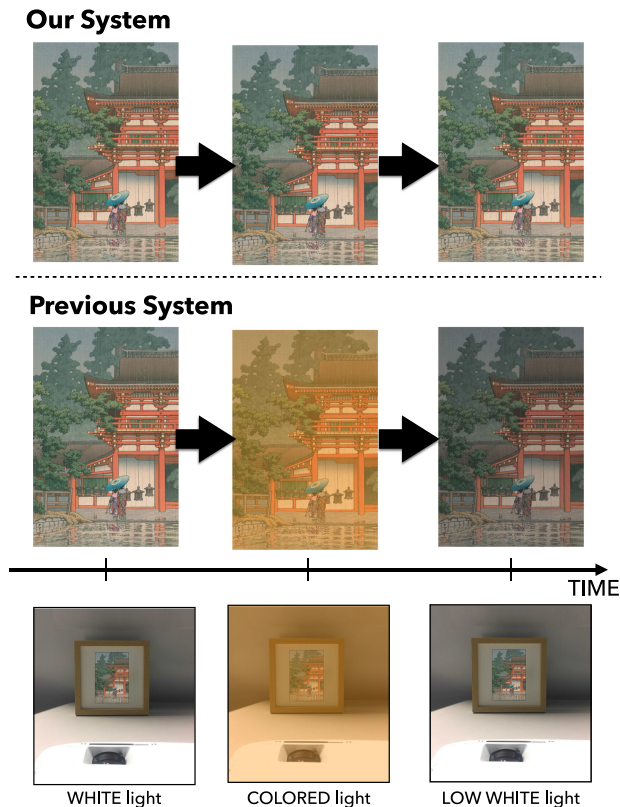


Fig. 1. Estimated original appearance of a painting, as determined by our system and the previous system under three lighting conditions: White light, colored light, and low white light.

In the present study, we develop a means to estimate the reflectance robustly under dynamic environmental light for appearance control with a projector–camera system. The basic concept on which this study is based is shown in Fig. 1. With our method, a projector–camera system can estimate the original appearance of a painting regardless of the environmental light, while previous methods would be adversely affected by changes in light. We created this method by improving on the reflectance estimation method by Amano et al. [11]. Henceforth, in this paper, we will refer to the method devised by Amano et al. [11] as “the previous method.” With our improvement, the appearance control system can be applied in both static and dynamically changing lighting conditions. As a result, the system is capable of the following:

- The appearance control system can be utilized even when both the reflectance and environmental light are dynamically changing.
- Colors can be presented exactly as desired when the color is inside the presentable range of a projector. The previous method could only present relative colors.
- The system can continue to operate as expected without additional calibration, even when the lighting conditions change.

We describe these contributions in greater detail in Section 5.

2 RELATED WORK

Nayar et al. [12] and Grossberg et al. [13] designed methods of optical compensation for static situations. In these

studies, a projection onto a colored surface appeared as if it were on a white screen. Grundhofer et al. [14] established a method to reproduce high-contrast images in a projected display by considering the properties of human vision. Brown et al. [15] created a model based on the characteristics of projectors and the object onto which an image was being projected to control the brightness of the display produced by a multiprojector system. These techniques require prior knowledge of the reflection characteristics of the target objects. In other words, we cannot move the target object, and the environmental light also needs to be constant.

By improving these techniques, Fujii et al. [16] designed another optical compensation method that can be applied when the target objects are moving. Tsukamoto et al. [17] designed an optical compensation system based on a multiprojector–camera system. They considered the calculation and communication cost and implemented a system to which more cameras or projectors can easily be added. Mihara et al. [18] designed a radiometric compensation technique that is effective for projecting light onto steep reflecting objects. These techniques can adjust the projection color even when the target objects and environmental light are dynamically changing. Pjanic et al. [19] created a system using a galvanoscopic laser projector (GLP) and normal video projector, in which the GLP was used to reproduce the colors that cannot be reproduced by the normal projector. The objective of all of these studies was to enable the reproduction of the original colors of digital content as they would appear when observed under white light. Therefore, these systems relied on target images and adjusted the colors of the reflected light to match those of the target images. The appearance control system reproduces target images using a feedback mechanism. This is the main difference between optical compensation techniques and appearance control techniques, including that devised in the present study.

In contrast to optical compensation, many studies have attempted to control the appearance of a target object by overlaying a projection based on the original appearance of the target object. The fundamental technology of appearance control is same as that of optical compensation. Appearance control technology also controls the light projected onto a real object at the pixel level. In the initial stages, projection technology must acquire the appearance of an object in advance and under white light. In other words, it can only be used in static situations [20], [21]. To introduce a feedback structure to appearance enhancement, Amano et al. [22] and Bimber et al. [23], [24] designed a real-time appearance control algorithm that does not require an object’s original appearance to be precaptured. By adapting control theory, Amano et al. [11], [25] dynamically control the appearance control that employed a model predictive control (MPC) algorithm. Recently, some research has focused on the manipulation of material perception by light projection [26], [27]. In the present study, we devised a means of estimating the reflectance for appearance control.

In this paper, we propose a method for estimating the reflectance of a target object as required for appearance control with a projector–camera system. Previous studies that have addressed appearance control as a means of manipulating the colors of objects required knowledge of the reflectance

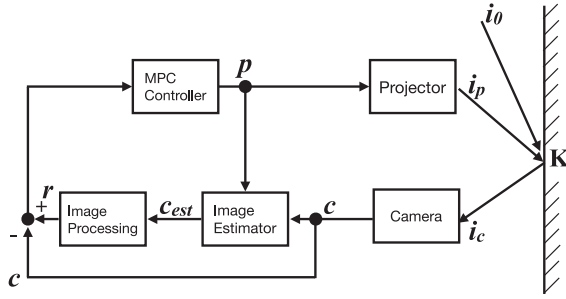


Fig. 2. Appearance control method by Amano et al. [11].

of the object. Conventional methods can estimate the reflectance of dynamic objects in real time; however, they assume that the environmental light is constant. With our method, an appearance control system can be applied even when both the reflectance and environmental light are dynamically changing. Our preliminary trials suggest that our idea has the potential to robustly estimate the reflectance in a dynamic light environment [28]. In this study, we appended a more generalized method to increase the number of potential applications. Furthermore, we conducted experiments to evaluate our method with a projector–camera system that we implemented.

3 ROBUST REFLECTANCE ESTIMATION

In this section, we explain our method for estimating the reflectance using a projector–camera system. First, we discuss estimation under static environmental light conditions, as described by Amano et al. [11]. Second, we explain our method that can robustly estimate the reflectance under dynamic environmental light conditions. There are several ways to implement a projector–camera system that is capable of implementing our method. Herein, we explain our estimation method assuming the use of two cameras. Finally, we explain the control theory employed in our system to realize convergent projection.

3.1 Reflectance Estimation in a Static Light Environment

Amano et al. [11] estimated the reflectance of each pixel as well as the changes in the appearance of the objects' surfaces using a projector–camera system with a single projector and single camera, as shown in Fig. 2. The light i_p from the projector and the constant environmental light i_0 are reflected by the surfaces, for which the reflectance is \mathbf{K} . The light captured by the camera i_c consists of the reflected light of i_p and i_0 . This system regards i_c as the same as the light captured by a human eye. i_c is expressed as follows:

$$i_c = \mathbf{K}(i_p + i_0). \quad (1)$$

An image c captured by the camera is expressed by the following model:

$$c = \mathbf{K}\{(c_{full} - c_0) \odot p + c_0\}, \quad (2)$$

where p is the projected image, \mathbf{K} is the reflectance of each pixel, and c_{full} and c_0 are the captured images with the maximum and minimum power projections, respectively. \odot

means the element-wise multiplication. In (2), the color space conversion process is omitted. When we display one color with a projector and capture the projection with a camera, the pixel values of the projection and captured images are usually different. This is because each device has its own color space. In order to treat these images with same equation, their color spaces must match. To achieve this, we utilize a color-conversion matrix to convert from one color space to another. In photometric calibration, a projector sequentially displays red, green, and blue images on a white plane, and a camera captures the projection. With three projection images and three captured images, we can calculate the color-conversion matrix between the projector and the camera. We assume that the geometric and photometric calibration between a camera and a projector has already been completed. We do not attempt to incorporate geometrical and color conversion into the equations at this point. In (2), the only unknown parameter is \mathbf{K} . Therefore, \mathbf{K} can be estimated as $\hat{\mathbf{K}}$ using

$$\hat{\mathbf{K}} = \text{diag}[c./\{(c_{full} - c_0) \odot p + c_0\}], \quad (3)$$

where $./$ is the element-wise division.

The original appearance of a target object c_{est} , i.e., the appearance under white light, can be estimated on the basis of the reflectance $\hat{\mathbf{K}}$ and a projected white image $c_{white} = (1, 1, 1)^T$

$$c_{est} = \hat{\mathbf{K}}c_{white}. \quad (4)$$

After the original appearance c_{est} is estimated, a reference image r is created by adding some effects, such as color saturation enhancement or color phase shifting, to c_{est} . Then, the system calculates the difference between the reference image r and current appearance c in order to create a negative-feedback loop.

3.2 Reflectance Estimation in a Dynamic Light Environment

To estimate the reflectance in a dynamic light environment, it is necessary to simultaneously estimate both the reflectance and environmental light. Our concept involves the creation of two different light conditions that alternate very quickly such that they are not perceived by the human eye. Images of objects under each light condition are captured. The idea of embedding different images within consecutive projection frames has been proposed in many spatial augmented reality studies [29], [30], [31]. The light conditions i_1 and i_2 are respectively expressed as

$$i_1 = \mathbf{K}(i_{p1} + i_0 + i_f), \quad (5)$$

$$i_2 = \mathbf{K}(i_{p2} + i_0 + i_f), \quad (6)$$

where $\mathbf{K} \in R^{3 \times 3}$ is the reflectance of each pixel, $i_{p1}, i_{p2} \in R^3$ is the light from the projector, $i_0 \in R^3$ is the environmental light when the system is calibrated, and $i_f \in R^3$ is the variation in the environmental light from i_0 . i_p, i_0 , and i_f are reflected from the objects' surfaces, and the camera captures the reflected light. By switching i_{p1} and i_{p2} at a high speed, the human eye perceives the combination of i_{p1} and i_{p2} as

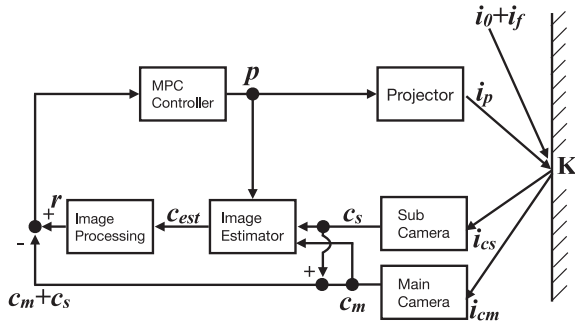


Fig. 3. Our appearance control method using two cameras.

the projected light. When two colors are switched faster than the critical flicker frequency (CFF), the human eye perceives the average color of the two [32], [33]. By creating two light conditions by switching the projection, we can capture two types of reflected light, which an observer cannot perceive.

We added a new parameter—“environmental light f' ”—to (3) to represent the captured images of i_1 and i_2 on the basis of (5) and (6). In the following, we assume that the geometric relationship between the camera and the projector is already known and that the camera pixels correspond to the projector pixels on a one-to-one basis. In addition, if both i_{p1} and i_{p2} are chromatic, we must consider the mixture of the colors, which makes the problem complex. We set $i_{p2} = (0, 0, 0)^T$ to avoid this complexity, such that we only have to consider the brightness. The captured images of i_1 and i_2 are expressed as

$$c_1 = \mathbf{K}\{(c_{full} - c_0) \odot p + c_0 + f\}, \quad (7)$$

$$c_2 = \mathbf{K}(c_0 + f), \quad (8)$$

where c_1 and c_2 are the captured images of i_1 and i_2 , respectively. From (7) and (8), the reflectance \mathbf{K} can be estimated by considering the change in the environmental light according to

$$\hat{\mathbf{K}} = \text{diag}[(c_1 - c_2) ./ \{(c_{full} - c_0) \odot p\}]. \quad (9)$$

In addition, the environmental light \hat{f} and reflectance $\hat{\mathbf{K}}$ can be simultaneously estimated using (8) and (9)

$$\hat{f} = \hat{\mathbf{K}}^{-1}c_2 - c_0. \quad (10)$$

3.3 Separation of Environmental Light Using Two Cameras

When the projector–camera system consists of a single camera and single projector, the reflectance can be estimated using (9). However, when the system incorporates two cameras, we must also consider their geometrical relationship and color spaces. In this section, we explain our method of reflectance estimation using two cameras that matches the geometric relationship and color spaces between two cameras. The light paths and processing flow are shown in Fig. 3.

First, we explain how we match the geometrical relationship between the devices. The viewpoints of the cameras cannot be the same unless the cameras and projectors are

coaxial. Therefore, we need to convert the two different viewpoints to a single viewpoint. We refer to one camera as the “main camera” and the other as the “subcamera,” and we convert the viewpoint of the subcamera to that of the main camera. The geometric relationships between each pixel of the “main camera and projector” and each pixel of the “subcamera and projector” are determined by gray code pattern projection [34]. Using these two relationships, we can calculate the relationship between each pixel of the main camera and each pixel of the subcamera, while the viewpoint of the images can be converted from that of the subcamera to that of the main camera.

The system is also required to apply a color-conversion matrix to match the color spaces of the devices. Each device has its own color space, with captured or projected images being represented within that color space. To represent all of the images in the same color space, the color-conversion matrix must be applied to those images. We convert the color space of the subcamera to that of the main camera using the following equation:

$$c_s' = \mathbf{M}_{ms}c_s, \quad (11)$$

where c_s is the image captured by the subcamera, and c_s' is the image captured by the subcamera, which is converted to the color space of the main camera. The image captured by the subcamera c_s is converted to and represented in the color space of the main camera $\mathbf{M}_{ms}c_s$. \mathbf{M}_{ms} is the color-conversion matrix that converts the color space of the subcamera to that of the main camera. We already have the color-conversion matrix between the main camera and the projector and that between the subcamera and the projector, as determined by photometric calibration. With these two matrices, we can easily calculate a color-conversion matrix between the main camera and the subcamera. When considering the color conversion from the subcamera to the main camera, we can rewrite (7) and (8) as

$$c_m = \mathbf{K}\{(c_{mfull} - c_{m0}) \odot p + c_{m0} + f\}, \quad (12)$$

$$\mathbf{M}_{ms}c_s = \mathbf{K}(\mathbf{M}_{ms}c_{s0} + \mathbf{M}_{ms}f'), \quad (13)$$

where c_m is the image captured by the main camera. c_{mfull} is the image captured by the main camera with maximum power projection. c_{m0} and c_{s0} are the images captured by the main camera and subcamera with minimum power projection, respectively. f' is the environmental light represented in the color space of the subcamera. We assure that $f = \mathbf{M}_{ms}f'$. All of the elements of (12) are represented in the color space of the main camera, while the elements in (13) are converted to the color space of the main camera through the application of the color-conversion matrix \mathbf{M}_{ms} . From (12) and (13), the reflectance $\hat{\mathbf{K}}$ can be estimated as

$$\hat{\mathbf{K}} = (c_m - \mathbf{M}_{ms}c_s) ./ \{(c_{mfull} - c_{m0}) \odot p\}. \quad (14)$$

The environmental light f can also be estimated using (13) and (14) in the same way as when only one camera is used

$$\hat{f} = \hat{\mathbf{K}}^{-1}\mathbf{M}_{ms}c_s - \mathbf{M}_{ms}c_{s0}. \quad (15)$$

Furthermore, if the subcamera is calibrated and we can assume that the color spaces of the main and subcameras are identical, (14) and (15) become the same as (9) and (10), respectively.

3.4 Model Predictive Control

Model Predictive Control (MPC) is a process control theory that was developed in the late 1980s. Dynamic adaptation [16] can be regarded as an MPC method. However, it cannot be easily applied to appearance control because it was designed to adjust the brightness of a projection onto a surface. Amano et al. [11] designed an appearance control system that calculates the reference trajectory and modeling errors using a negative-feedback loop. By applying MPC, the quality and robustness of their system are improved. In the present study, we used the MPC algorithm devised by Amano et al. [11].

To apply the MPC algorithm, we used the following projector response model

$$c_M(t+1) = \hat{\mathbf{K}}\{(c_{full} - c_0) \odot p(t+1) + c_0 + f(t+1)\}, \quad (16)$$

where $p(t)$ and $c(t) \in ([0, 1], [0, 1], [0, 1])$ are the normalized projection pattern and image captured at step t . We created the projection response model defined in (16) by adding environmental light f to the model developed by Amano et al. [11]. This model is used to determine the projection required to attain convergence. Thus, this model must contain the projection p . In the MPC process, we only focus on the images captured by the main camera (c_1 in Section 3.2 or c_m in Section 3.3), as indicated by c_M . The image prediction $c_p(t) \in R^3$ that contains the model error $e(t) \in R^3$ is expressed as

$$c_p(t+1) = c_M(t+1) + e(t), \quad (17)$$

where

$$e(t) = c(t) - c_M(t), \quad (18)$$

and the reference trajectory is

$$c_R(t+1) = \alpha c(t) + (1 - \alpha)r(t+1), \quad (19)$$

where α is tuning parameter and $r(t)$ is a reference image that is created based on an estimated original appearance. From (16), (19), and the control law $c_p(t+1) = c_R(t+1)$, we can acquire the manipulation value

$$\begin{aligned} p(t+1) &= \hat{\mathbf{K}}(t)^{-1}(1 - \alpha)\{r(t+1) - r(t)\} / (c_{full} - c_0) \\ &\quad + \hat{\mathbf{K}}(t)^{-1}\hat{\mathbf{K}}(t-1)\{c_0 + f(t)\} - c_0 - f(t+1) \\ &\approx \hat{\mathbf{K}}(t)^{-1}(1 - \alpha)\{r(t+1) - c(t)\} / (c_{full} - c_0) + p(t). \end{aligned} \quad (20)$$

Although we added the environmental light f , it is eliminated in (20). Therefore, the system can predict the projection p without any influence from the environmental light.

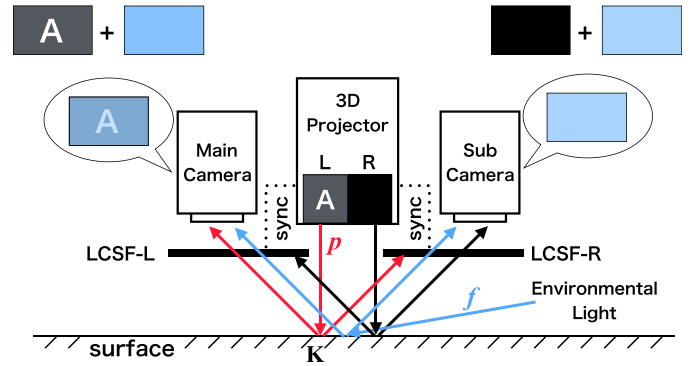


Fig. 4. System structure and light from a projector and the environment.

4 EVALUATION

In this section, we present our experiments to demonstrate that our method can robustly estimate the reflectance as the environmental light changes. First, we explain how we implemented the system. Then, we explain the experiments that we used to evaluate our method.

4.1 Implementation

In this section, we explain how we implemented the projector-camera system used in our experiments. First, we explain the two ways in which we capture images that are alternately projected from a high-speed projector. Second, we explain how we simulated the image captured by the human eye.

4.1.1 System Implementation

To apply our reflectance estimation method, it is necessary to capture two different images that are alternately projected by a high-speed projector. There are two ways in which this can be achieved: 1) using two cameras, a projector, and liquid-crystal shutter filters (LCSFs) that are synchronized with the projector and 2) synchronizing a camera with the projector. We implemented both systems to confirm that they can both capture two projections separately. In this section, we explain how these systems were implemented.

First, we will explain how we implemented the projector-camera system with two cameras. The system consists of two cameras, a three-dimensional (3D) projector, and a liquid-crystal shutter filter. Fig. 4 shows the system structure and light paths. LCSFs are commonly used in 3D glasses, which allow us to watch 3D digital content. The LCSFs synchronize with a 3D projector, which alternately projects two different images at 120 Hz. There are two types of LCSFs, each allowing only one image to pass while blocking the other image. In our system, we attached the filters to the cameras to capture images under the two different lighting conditions. In particular, the 3D projector alternately projects images for appearance control and a black image (almost no projection). The LCSF that cuts off the images for appearance control is attached to the subcamera. With this filter installed, the subcamera only captures the reflected environmental light. The other LCSF is attached to the main camera, which captures the reflected projected light. We will explain this in greater detail in the next section.

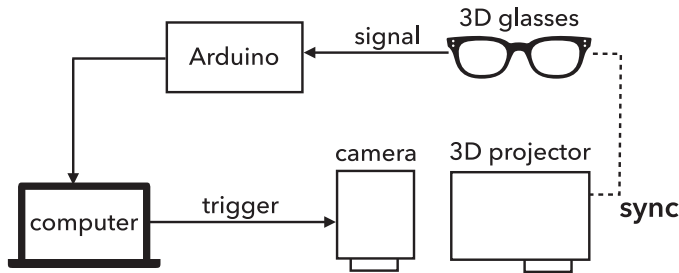


Fig. 5. Synchronization process between a camera and a projector.

To synchronize the camera and a projector, we also used a 3D projector and LCSFs to obtain the timings at which the projection switches. This synchronization is illustrated in Fig. 5. The 3D projector and 3D glasses are synchronized; the 3D glasses open/close in response to a command from the projector. Thus, we can acquire information about the projection timing by obtaining the signal from the 3D glasses. An Arduino microcomputer receives a signal from the 3D glasses and then sends it to a computer over a USB connection. Then, the computer sends a trigger to the camera at the timing at which the projection switches. The 3D projection is switched at a frequency of 120 Hz. Thus, after obtaining several timings, the camera can capture both projections by simply maintaining the framerate at 120 Hz. Fig. 7 shows the images captured with each implementation. With a 120 Hz projector, we alternately projected two types of images, and a camera (or two cameras) separately captured the projected images. We confirmed that both implementations are effective for capturing projections separately. In our experiments, we used a projector-camera system that consists of two cameras and one projector. This is because it is necessary to consider the geometry and color conversion between two cameras, which is not necessary in the implementation of one camera and one projector. The conversion may cause errors in the estimate of the reflectance. Thus, we select this implementation to ensure both implementations are effective for estimating the reflectance.

Fig. 6 shows our system and a target area. The cameras are located close to the projector such that a large space can be used as the target area. We used the planar surface of a board placed in front of the system with a sheet of white paper attached to it to act as the target area. We assumed that the target surface is a Lambertian surface. Therefore, we used an inkjet printer to print a defined target object on the paper. We installed the projector parallel to the floor, while the board was perpendicular to the projector's optical axis.

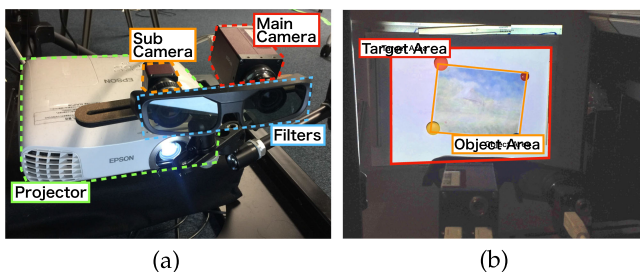


Fig. 6. System overview. (a) Projector and two cameras with filters. (b) Projected surface.

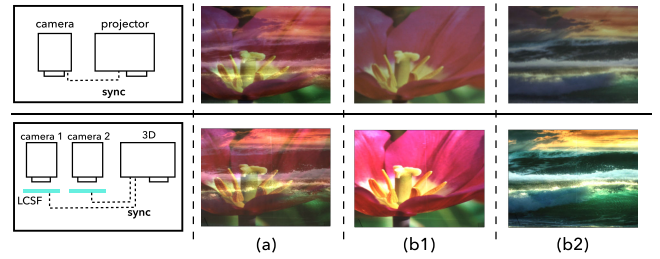


Fig. 7. Images captured by each implementation. The images in the first row are captured by the camera synchronized to the projector. The images in the second row are captured by the camera through LCSFs synchronized to the projector. (a) Images captured with a slow shutter speed. The two images overlap. (b1), (b2) Images captured at the appropriate timing with a high shutter speed. The two images are separated.

The equipment was as follows: Allied Vision PIKE (main camera), Allied Vision Guppy PRO (subcamera), EPSON EH-TW5200 (3D projector), MacBook Pro (computer equipped with an Intel Core i7 2.7 GHz CPU). We used C++ with the OpenCV and OpenGL libraries to implement the system.

4.1.2 Effects of Filters on the Captured Images

The images captured by the cameras with the LCSFs are darker than those captured without the LCSFs because the filters open/close. We attached an LCSF to both the subcamera and main camera. This was because we wanted to make the conditions under which the images were captured by the two cameras as similar as possible.

Amano et al. [11] assumed that the light captured by a camera is the same as that captured by the human eye. However, we cannot make this assumption. Each camera in our system captures light that has passed through an LCSF. Therefore, the light captured by the cameras is not that same as that captured by the human eye. The light captured by the main camera, subcamera, and human eye is shown in Fig. 8. We estimate the light to human eyes by calculating captured images of main and subcameras. The image seen by a human c_h can be represented by following equation:

$$\hat{c}_h = \frac{1}{2}(c_m + M_{ms}c_s). \quad (21)$$

Therefore, we need to consider the brightness at any given instant. The images captured by the main camera and

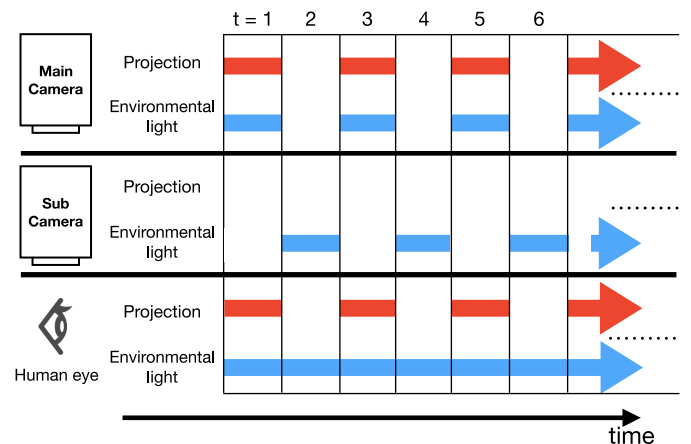


Fig. 8. Light captured by the main camera, subcamera, and human eye.

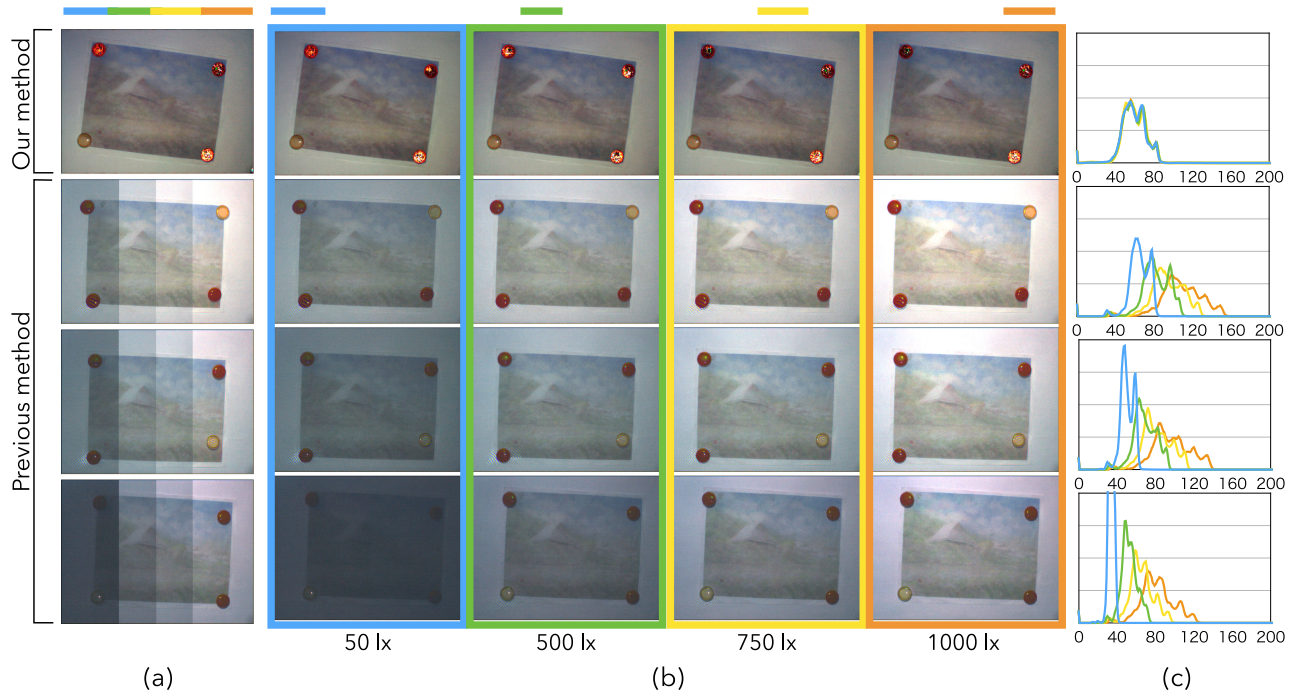


Fig. 9. Results of Experiment 1. (a) Combination of four slices from each estimated result. From the left, the estimated result at 50, 500, 750, and 1,000 lx, respectively. (b) Estimated original color under conditions with varying environmental light. (c) Brightness histograms for each image. Each color of the histogram corresponds to the color of the frame. The brightness values of these images are multiplied by 1.5.

subcamera are added together. This means that the result of adding the two images contains light from two units of time. Therefore, in the algorithm, we divided the sum by two to attain an amount \hat{c}_h that would be the same as that captured by the human eye. This estimate of c_h is also necessary for the implementation with one projector and one camera.

4.1.3 Controlling the Environmental Light

To test the robustness of our system, we needed a means of controlling the environmental light striking a target surface. To achieve this, we added another projector to simulate the environmental light in the experiment. Using this extra projector, we could project light with various colors and brightnesses. In Experiment 1, we used the extra projector to control the brightness of the light, while in Experiment 2, we used it to control the color saturation.

4.2 Experiment 1: Brightness

The goal of this experiment was to confirm that our method can robustly estimate the reflectance when the brightness of the environmental light changes. In addition, we estimated the reflectance using the previous method, which does not account for changes in the environmental light. This was done so that we could compare the results, which would confirm that our method produces superior results to those obtained with the previous method.

We measured the illuminance in our laboratory with a luminometer (Shinwa Rules, 78604 EYE HEALTH) at fixed intervals and reproduced the illuminance by using a projector. The brightnesses of the environmental light in the morning, afternoon, and evening were 750, 1,000, and 500 lx, respectively. We tested whether our method and the previous method could estimate the reflectance under simulated

environmental light produced by the other projector. Prior to applying our method, we calibrated the system at 750 lx, which is the brightness of the environmental light in the morning. Prior to applying the previous method, we calibrated the previous system using white light with brightnesses of 500, 750, and 1,000 lx. After calibration, we adjusted the brightness of the environmental light to 50, 500, 750, and 1,000 lx. We compared the estimated reflectances obtained using our method and the previous method. In addition, we also created a brightness histogram for comparison.

Figs. 9a and 9b show images of the estimated original appearance under white light. Fig. 9c shows a histogram of the brightness. Each color in the histogram corresponds to each color of the frame surrounding the images. The images in the first row were evaluated using our method after it had been calibrated using 750-lx environmental light. The images in the second, third, and fourth rows were estimated using the previous method after it had been calibrated at 500, 750, and 1,000 lx, respectively. The results obtained with our method remain constant even as the brightness of the environmental light increases. However, with the previous method, the results increase as the brightness of the environmental light increases. This can also be determined from the histograms. There are four histograms for the graphs shown in the second, third, and fourth rows, while there is only one histogram for the entire first row. Every histogram in the second, third, and fourth rows is different because the results are affected by the amount of environmental light. However, when using our method, the histogram remains constant. On the basis of these results, we can say that our method can robustly estimate the reflectance despite changes in the brightness of the environmental light, unlike the previous method.

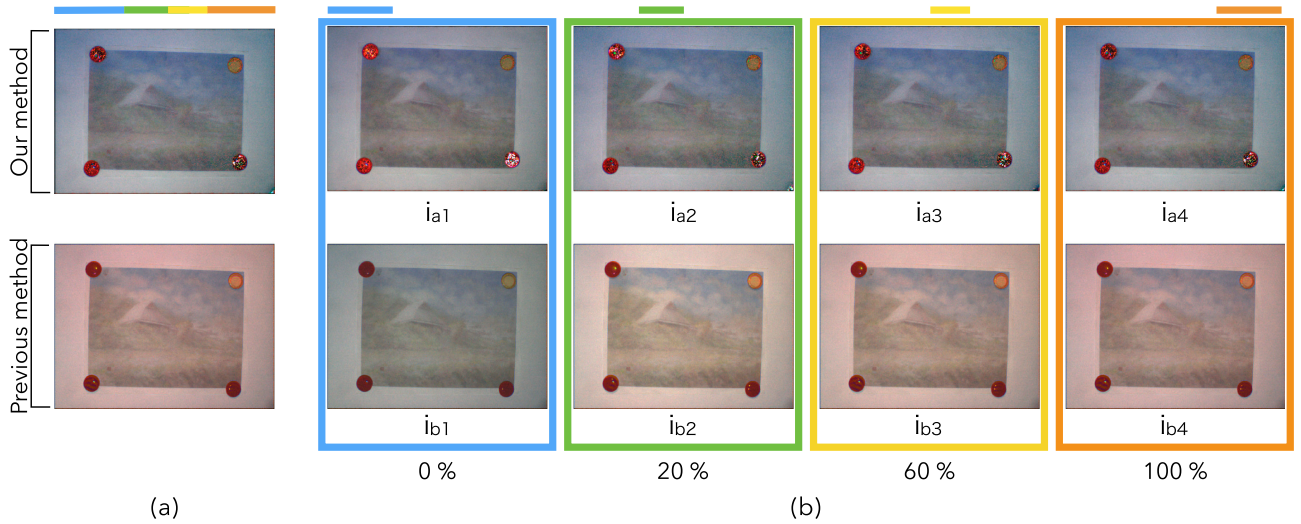


Fig. 10. Results of Experiment 2. (a) Combination of four slices from each estimated result. From the left, estimated result under environmental light with 0, 20, 60, 100 percent color saturation, respectively. (b) Estimation results for the original appearance under orange-colored environmental light. i_{a1} – i_{a4} are estimated by our method, and i_{b1} – i_{b4} are estimated by the previous method. The brightness values of these images are multiplied by 1.5.

4.3 Experiment 2: Color Saturation

The goal of this experiment was to confirm that our method is capable of robustly estimating the reflectance when the color saturation of the environmental light changes. We also estimated the reflectance using the previous method in the same way as in Experiment 1.

In practice, the color of the environmental light is often orange, such as sunlight at dusk or the light from an incandescent lamp. Therefore, for this experiment, we chose to use an orange light to simulate the environmental light. After photometric calibration under white environmental light, we changed the color of the environmental light to orange with a hue of 36 degree using another projector. We then compared the results estimated with our method and the previous method for a range of saturations of colored environmental light.

Fig. 10 shows the results of this experiment. The upper images (i_{a1} – i_{a4}) were obtained using our method, while the lower images (i_{b1} – i_{b4}) were estimated using the previous method. i_{a1} and i_{b1} were estimated under 0 percent color saturation, i_{a2} and i_{b2} under 20 percent, i_{a3} and i_{b3} under 60 percent, and i_{a4} and i_{b4} under 100 percent. Although the

results obtained with the previous method assumed an orange color as the color saturation increased, the results obtained with our method remained constant.

We converted the color space of all of the estimated results from red, green, and blue (RGB) to Lab and calculated the mean value of a^* and b^* for each image. Using these values, we calculated the distance for each image on the a^*b^* plane. In particular, we calculated the distance between the image estimated using our method under calibrated light (i_{a1}) and the other images that were estimated using our method under colored environmental light. The same calculation was also applied to the images estimated by the previous method. Fig. 11 shows a graph of the calculated distances. Although the values obtained with the previous method are larger when the color saturation is higher, the value obtained with our method remains constant at around 1. This result demonstrates that, relative to the previous method, our method can robustly estimate the reflectance when the color saturation of the environmental light changes.

4.4 Experiment 3: Reflectance Estimation for a Complex Environmental Light Pattern

The goal of this experiment was to confirm that our method can robustly estimate the reflectance of various objects for a range of environmental light levels while comparing it with the previous method. We prepared three objects as targets and four images with different levels of environmental light, which are shown in Fig. 13. We estimated the reflectance for every combination using our method and the previous method. For this experiment, we changed the subcamera to a Point Grey Flea 2 camera. The estimated results are shown in Fig. 12. In addition, we calculated the difference between the corresponding pixel values of the estimated and captured images under white illumination, and we created box plots in RGB individually. We performed an one-sided t-test between the data for each box plot (99 percent confidence interval). The results of the t-test are also shown in Fig. 12.

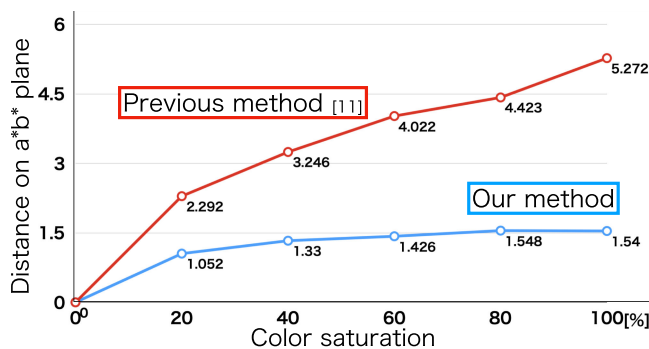


Fig. 11. Distance between the mean value of the estimated result obtained under calibrated light and the result obtained under colored light on the a^*b^* plane. The red line indicates the results obtained with the previous method [11], while the blue line shows the results obtained with our method.

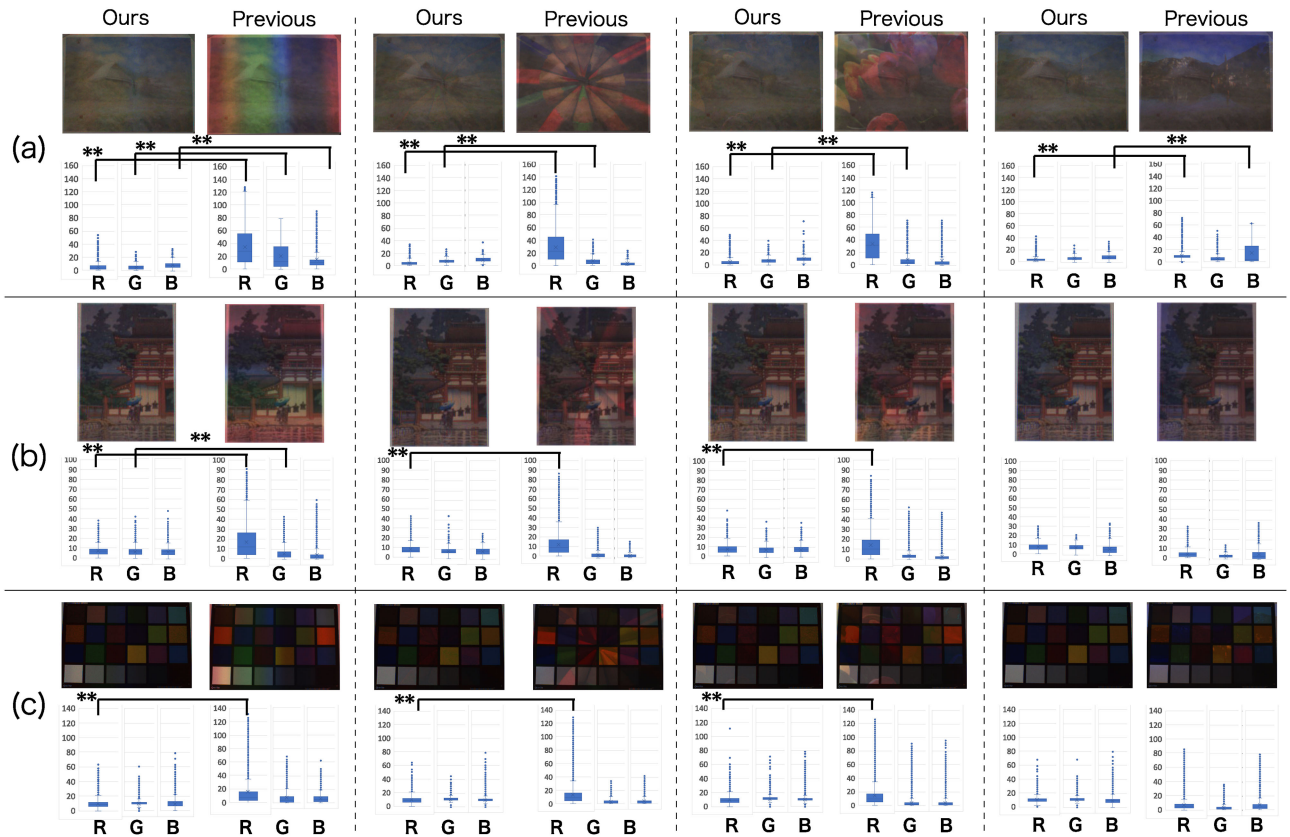


Fig. 12. Results of Experiment 3. (a), (b), and (c) show the estimated results of different objects. The left images in each pair are the results estimated by our method, and the right images are those estimated by the previous method. **: p value < 0.01 .

4.5 Experiment 4: Accuracy of the Controlled Results

In this section, we compare the reference images and controlled results obtained with the system to determine whether our system can accurately change the appearance of an object from the original appearance to the target appearance. We used the same objects as those used in Experiment 3 but presented them in monochrome. The reference images and controlled-appearance images are shown in Fig. 14. We created a heat map of the difference images for each RGB pair to better visualize the results. In addition, we calculated the mean squared error (MSE) of each difference image. For (a) and (b), the two images are almost completely the same. We can determine this both visually and from the very low

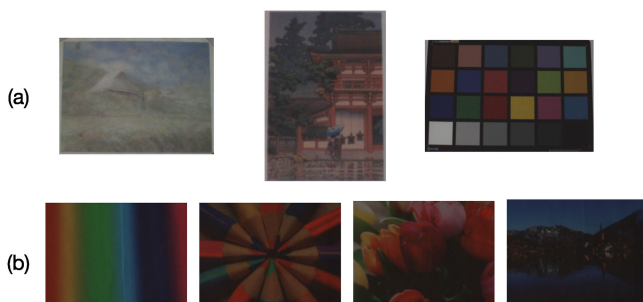


Fig. 13. Target objects and environmental light patterns used in Experiment 3. (a) Images of three objects captured under white illumination. (b) Four environmental light patterns.

MSEs for every channel. However, for (c), some areas in the controlled-appearance image retain their colors slightly. This can be also be determined from the heat maps. In the heat map for the blue channel of (c), we can observe at least four such areas, while the MSE was the highest for this experiment.

4.6 Experiment 5: Controlled Results

In this section, we present the controlled appearance produced by our projector-camera system. We used two types of projectors: a 3LCD projector (EPSON EH-TW5200) and a 1-chip DLP projector (BENQ TH671ST). The controlled results for four effects are shown in Figs. 16 and 17. The four effects are 1) color saturation enhancement, 2) color phase shift (two directions), 3) monochrome effect, and 4) texture reduction.

We also tested the control of the appearance of objects that have specular reflection characteristics. We scanned an X-rite color checker and printed the captured images on two types of glossy paper (FUJIFILM Photo paper WPA420PRM and FUJIFILM Photo paper Ultra Gloss WPA412PRO). The estimated results are shown in Fig. 15. Although the positions of the camera and projector play significant roles, the system can estimate their reflectance. The cameras were not placed at positions that can capture the specular component of the projected light. Thus, the system can estimate the reflectance. However, when we illuminated the surface with a flashlight, black and bright spots appear on the estimated images. These are caused by the specular components of the light

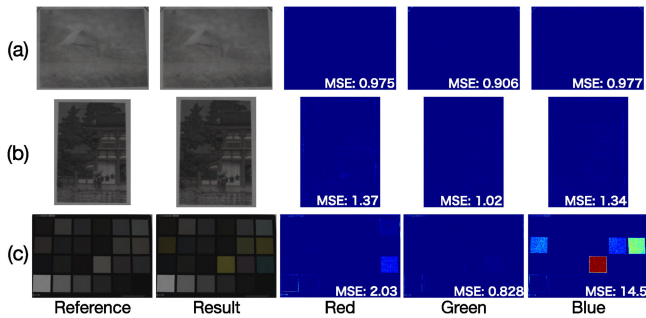


Fig. 14. Reference images and controlled results. The difference between each pair consisting of a reference image and a controlled result image is visualized as heat map. They are divided into RGB channels.

from the flashlight. The positions on the objects at which the specular components appear differ depending on the camera positions. Given that we used two cameras, two spots appear on the images.

5 DISCUSSION

The results of Experiment 1 imply that our system is capable of robustly estimating the reflectance even when the brightness of the environmental light changes from 50 to 1,000 lx. The recommended illuminance for a drafting space in an office or an operating room in a hospital is usually no more than 1,000 lx [35]. Therefore, when our system is applied indoors, it operates as expected. However, the illuminance outdoors often reaches 100,000 lx at noon. Under this type of illumination, we would not expect our system to be capable of estimating the reflectance. This is because the camera cannot capture the light coming from the projector in such a bright environment. Similarly, the human eye cannot see the projected light in the presence of strong sunlight. Thus, even if our system was able to estimate the reflectance, it would not be possible to project

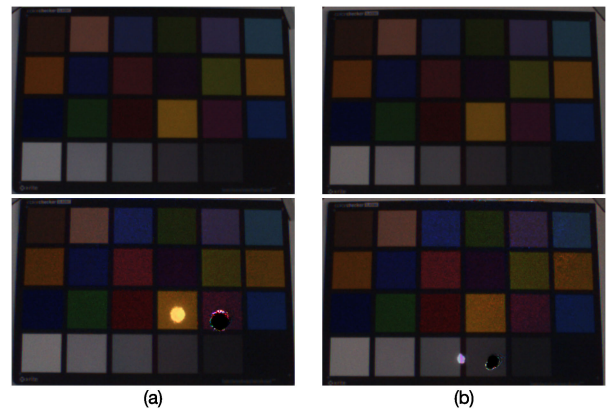


Fig. 15. Estimated results printed on (a) glossy paper (FUJIFILM Photo paper WPA420PRM) and (b) ultraglossy paper (FUJIFILM Photo paper Ultra Gloss WPA412PRO). The upper results are estimated under white indirect illumination, and the lower results are estimated under direct illumination.

images that would be visible when using a projector. Once the illuminance falls below 1,000 lx at dusk, our system can be applied outdoors. Therefore, we believe that our system's acceptable illuminance range is sufficiently broad for application to typical situations.

Given the results of Experiment 2, we conclude that our system can be used in an environment with colored light. The color of indoor light is not always white. For example, incandescent lamps often give off an orange hue. In addition, it is very easy to acquire equipment that can be used to control the color of indoor lights. Generally, the color saturation of indoor light is not very high. Even when the color saturation is high, we would not expect light equipment to irradiate colored light with 100 percent color saturation in the hue, saturation, and value (HSV) color space. In addition, in Experiment 2, we only performed a test with orange environmental light, but our system could theoretically be applied to an

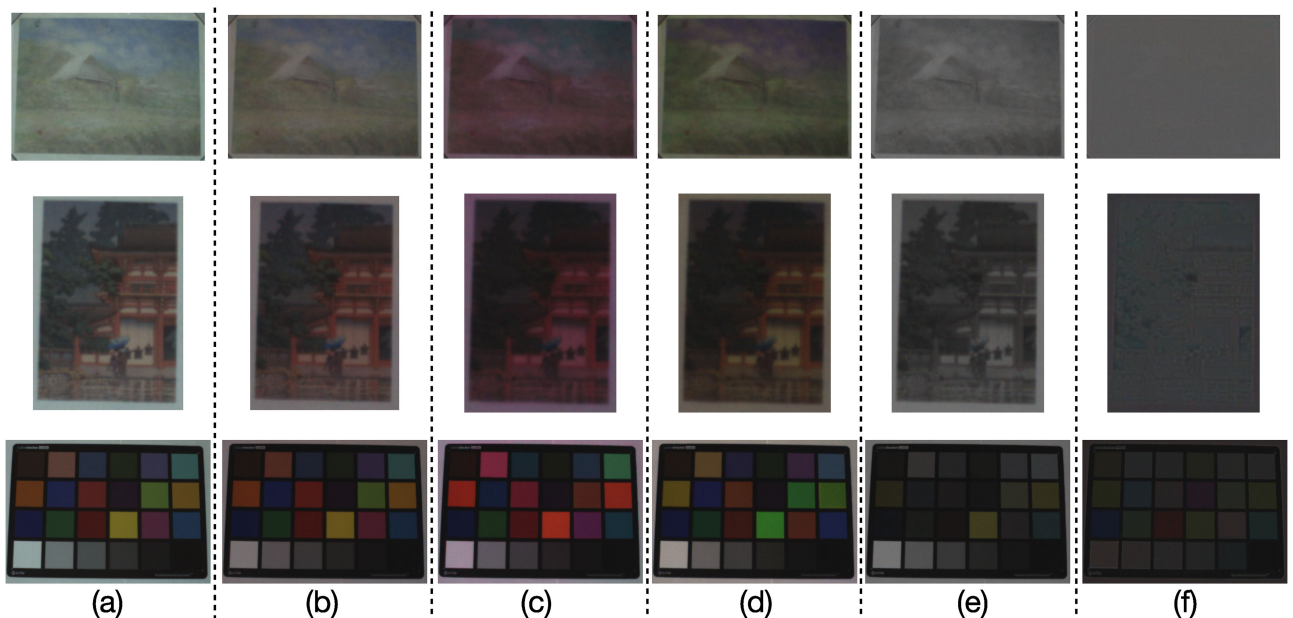


Fig. 16. Controlled appearance with the system using a 3LCD projector: (a) Original appearance, (b) color saturation enhancement, (c) color phase shift +, (d) color phase shift -, (e) monochrome effect, and (f) texture reduction. The brightness values of images (b)–(f) are multiplied by 2.0.

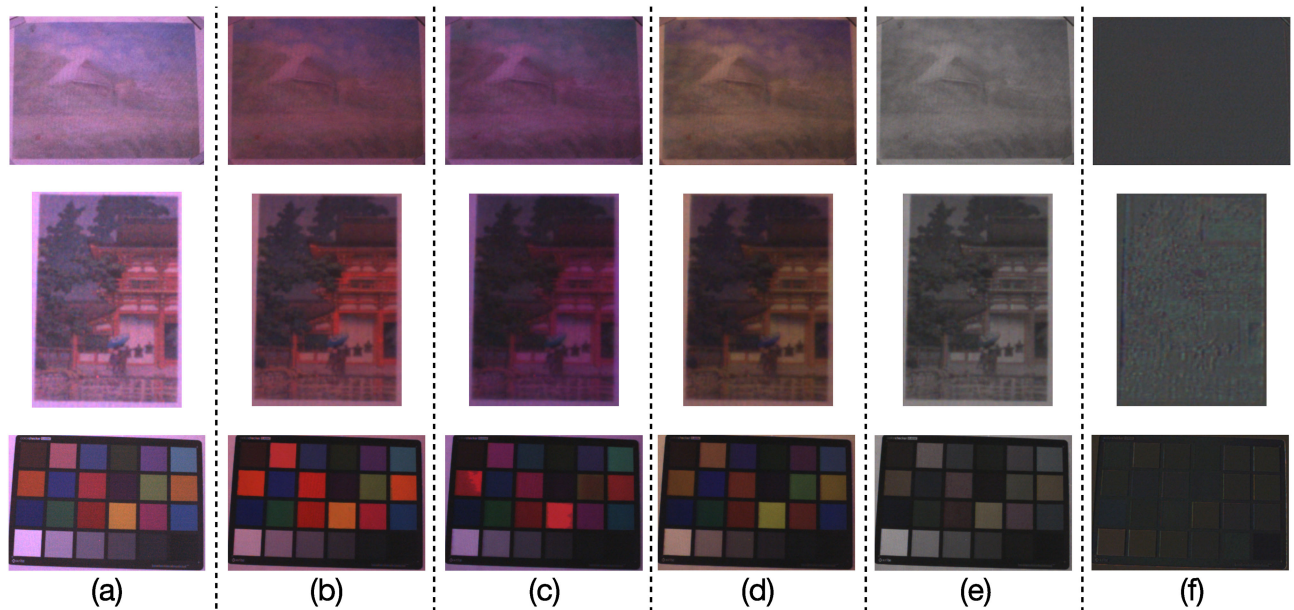


Fig. 17. Controlled appearance with the system using a DLP projector: (a) Original appearance, (b) color saturation enhancement, (c) color phase shift +, (d) color phase shift -, (e) monochrome effect, and (f) texture reduction. The brightness values of images (b)–(f) are multiplied by 2.0.

environment with light of any color. Therefore, we feel that the acceptable color range of our system is also sufficiently broad for practical use.

On the basis of the results of Experiment 3, we can state that our method can robustly estimate the reflectance even when the environmental light has complex brightness, color, and texture patterns. However, if we focus on each channel of the results, the previous method incurred smaller errors in some cases. For example, in the first result on the right in Fig. 12a, the environmental light pattern is mostly blue. Therefore, the results obtained with the previous method have larger errors than those incurred by our method for the blue channel. However, for the green channel, the results obtained with the previous method have smaller errors than those obtained with our new method. We believe that our method incurs a greater continuous error than the previous method. The calculations required by our method are more complex than those of the previous method, and we also use two cameras, both of which incur errors. In addition, in the box plots shown in Fig. 12c, the results obtained with the two methods appear very similar. We believe that this is a result of the color checker having very deep colors, such that its surface does not strongly reflect the environmental light patterns. In this case, the estimated results are not greatly affected by the environmental light patterns. However, when we visually compare the results obtained with the two methods, we can easily identify some edge patterns and uneven brightness or color areas in the results obtained with the previous method. This effect is barely visible in our box plots, which is a major improvement over the previous method.

On the basis of the results of Experiment 4, we conclude that our system can accurately control the appearance of objects relative to the reference images. In Figs. (a) and (b), the MSEs for every result are very low. However, in Fig. 14c, there are some areas that have errors. We believe that they are caused by the specifications of the projector. In

the heat map for the blue channel in (c), the original colors of the areas with larger errors are deep yellow and orange. The projector must project strong blue illumination onto these areas to make them monochrome. However, in this experimental setup, the projector cannot produce sufficiently bright blue illumination. Thus, we believe that our estimation and control processes are not the source of the errors. Rather, the errors are incurred by the lack of projector power.

In Experiment 5, we demonstrated the possibility of controlling the appearance of three objects with two projectors—namely, 3LCD and 1-chip DLP projectors. We think that our method can be applied irrespective of the type of projector. In addition, the controlled and estimated results for printed paper with strong specular reflection characteristics were also shown. These results show that our system can estimate the reflectance and control the appearance of objects having specular reflection. However, there are some limitations. First, the positions of the cameras and projector are limited. If the camera captures the specular reflection of the projection, the system cannot estimate the reflectance of that area. Additionally, the system cannot estimate the reflectance or control the appearance when the projected area is directly illuminated. In this case, the position and direction of the direct illumination also play a significant role, but the system loses control of that area when the cameras capture the specular reflection. In our experimental setup, we used two cameras, such that the positions of the specular reflection in the projected area differed between them. This is because there are two points (black and white) in the estimated results shown in Fig. 15. Although this is one of the limitations of our method, the information may be useful for other purposes such as estimation of the light source position. By using the positions of the specular reflection on the projected surface and the camera positions, we can estimate the position of the source of direct illumination.



Fig. 18. Appearance control with the canceling of additional light. Our system can make the colored area appear monochromatic. (a) Instant at which a red spotlight illuminates the object surface and (b) after the system compensates to eliminate the red light.

5.1 Contributions

The contributions of this work are 1) robust reflectance estimation despite dynamic changes in environmental light, 2) absolute color reproduction, and 3) calibration-less operation. In this section, we explain these contributions in greater detail.

Our first contribution is robust reflectance estimation despite dynamic changes in the environmental light. Our method can estimate the reflectance of a target object even when both the reflectance and environmental light are dynamically changing. For example, if we were to attach the system to a moving object, they would both be dynamic. Projectors are becoming smaller, and many studies have considered the attachment of a projector to a user's body [36] or vehicle such as a bicycle [37]. In addition, given its robust ability to estimate the reflectance, our method can overcome the effects of the variation in the environmental light. Of course, it can not only handle changes in the overall environmental light of a room but also handle spatial changes in the environmental light, as would occur with spotlights. In Fig. 18, the system eliminates the effect of the red spotlight, maintaining the monochrome appearance of the painting. It is also possible to change the color of spotted light while the colors of objects are controlled to be different. We think we can create a new user experience with our system. Additionally, when the projected area is large, the environmental light is not always spatially uniform because of the layout of the lighting equipment or the presence of a highly directional light source. Even in this situation, our method can handle the variation in the environmental light, such that the projected area appears as if it is under uniform environmental light.

Second, our method can reproduce absolute color. The human eye captures light that is reflected from objects and thus perceives colors. Thus, colors are determined by the reflectance and incident light. Even if a projector projects a given quality of light onto the same object, the reflected light will vary depending on the environmental light. Therefore, we need to know both the reflectance and level of the environmental light if we are to be able to reproduce absolute colors. Our system estimates both the reflectance and environmental light. The incident light consists of both environmental and projected light. Using this information, the desired colors can be reproduced without special lighting. This would be useful for designing tasks or the simulation of an appearance. For example, when we need to design a poster, we can try other colors after printing. Additionally, our system can simulate an appearance in an

environment with various colors of light, irrespective of the lighting conditions.

Finally, our method allows an appearance control system to be operated without the need for calibration. The appearance control system based on the previous method requires photometric calibration to be performed whenever there is a change in the environmental light. This is because the previous method focused only on short-term use and assumed that the environmental light would be constant. With our method, the appearance control system can be used over the long term without any additional calibration. Given the above, we believe that the appearance control system could be used as an intelligent light source capable of supporting human vision. Applications could include changing the color of letters that are difficult to read or making the colors of a faded photograph vivid. When used as an intelligent light source, we would expect users to keep the system turned on, in which case recalibration would be troublesome. Therefore, given that our method allows an appearance control system to operate without the need for calibration, it would make a major contribution to the use of the system as an intelligent light source.

5.2 Limitations

Our experiments revealed the limitations of the new system. First, when the colors of objects are dark or deep, the system sometimes cannot accurately control their appearance. This is a function of the color of the surface and the environmental light [38]. When the surface color is very dark, the light emitted by the projector is barely reflected by the surface. Thus, very powerful projection is required to give the appearance of many colors. However, with our method, the full power of the projector cannot be used because of switching during projection. Thus, the maximum brightness of the projector is halved. Because of this limitation, there are differences between the reference image and the controlled result, as shown in Fig. 14c. Therefore, fewer colors can be presented relative to projectors that do not switch the projection on and off.

Second, when we wanted to apply compensation for a colored spotlight, we found that our system is basically capable of doing so. However, the spotlight only became dimmer, with the color still visible in some parts of the target object. We believe that this is a function of the color space conversion between the main camera and subcamera. The system multiplies every pixel of the images captured by the subcamera by the matrix M_{ms} . Thus, color space conversion is applied equally even if the cameras fail to capture the scene uniformly, as in the case of vignetting.

In our implementation, the projector switches on/off at 120 Hz. The difference in the brightness between these two projected images is very large. This may lead to flicker perception for some observers. We prepared two projector-camera systems to examine the issue of flicker perception. One system switched the projection on/off at 120 Hz, while the other system did not. We placed the same printed objects in front of each system and used the system to control the appearances of the objects. We showed these controlled-appearance objects to participants and asked them to inform us if they felt that there were any differences between them. We performed this experiment using four

participants, all of whom noted slight flickering. We conjecture two reasons for this flickering perception in our experimental setup. The first reason is that the projection onto the white surface switches to bright white and black. As shown in Fig. 6b, we take a broader target area compared to the object area. In our algorithm, the system does not track the object, but it focuses on controlling the colors of each pixel. The target area except the object area is illuminated by white light if the surface is white. We regard the color of the background as white, and, in our algorithm, a nontarget region will be illuminated by white light. The difference in the two brightnesses of the flickering area is one of the reasons for flicker perception [39], [40]. The difference in the brightnesses between two projected images of the area becomes larger than that of the object area. In addition, there is greater perception of flicker when the size of the white projection area is larger [41]. We conjecture that this unnecessary white illumination leads to flicker perception. Though it is a subjective evaluation, we feel that flicker perception is reduced by limiting the projection area. Thus, we think that flicker perception can be reduced by tracking objects and limiting the projection region. It is also possible to solve this problem by projecting at a sufficiently high framerate at which humans cannot perceive flicker. Davis et al. [42] found that humans perceive flicker even at a frequency of 500 Hz if the projected images include high-frequency spatial edges, while we only projected at 120 Hz. We conjecture that this leads to the perception of flickering. There are studies employing high-speed projector-camera systems [43]. They succeeded in preventing flicker perception with these systems. Thus, by employing a projection system whose framerate is higher than 500 Hz, we may prevent flicker perception.

In our current implementation, we do not consider the temporal flickering of light sources. Our cameras in the implementation with LCSFs have a longer shutter speed for capturing the projected area temporally and uniformly. However, depending on the frequencies of the light sources, the flickering of the light sources appears in the captured images. In this case, the system cannot robustly estimate the reflectance in the presence of the external light. One way to solve this problem is to implement a system with devices having a higher framerate. By implementing high-speed devices, the cameras capture both the bright and dark moments of the environmental light. By a statistical process, the system can omit the captured images without environmental light.

6 CONCLUSION AND FUTURE WORK

In the present study, we devised a method for robustly estimating an object's reflectance despite dynamic changes in the environmental light as a basic technology for application to appearance control using a projector-camera system. Any such system requires the simultaneous estimation of both the reflectance and environmental light level. Our concept is based on the creation of two different light conditions, and images of the same scene are captured under these two conditions. To evaluate our method, it was implemented with a projector with a frame rate of 120 Hz, two cameras, and LCSFs. The results of the experiments

confirmed that our system can robustly estimate when the brightness and color of the environmental light change. We believe that the results of these experiments show that the system's resilience to brightness and color saturation is sufficient to allow its incorporation into indoor applications. The contributions of this study are 1) broadening the lighting conditions in which appearance control can be applied, 2) enabling the absolute presentation of colors, and 3) allowing appearance control to be implemented without the need for calibration. We also identified some limitations of our system. In situations in which the reflectance is very low, reflectance estimation become unstable. In addition, our system cannot compensate for the effect of environmental light in some areas because of the color space conversion between the two cameras.

In our future work, we intend to apply the system to 3D objects. Our system projects a gray code pattern onto a planar surface and creates a look-up table of each pixel for the cameras and projector to enable geometric calibration. Therefore, it should be possible to apply this system to a 3D object applying this calibration by projecting a gray code pattern directly onto the 3D object. However, the relationship between the pixels is lost when the 3D object moves, even at the pixel level. Thus, the currently implemented system will lose control as a result of the parallax effect between the cameras and the projector. This problem can be overcome by creating a projector-camera system in which the optical axes of the projector and camera are the same [44]. With a coaxial projector-camera system, the camera can ignore any specular reflection except in the center area. The projector radially projects light, and the camera is at an optically identical position to that of the projector. Thus, even if a target object has specular reflection characteristics, the specular reflection component is not returned to the camera, except for that part of the object that is perpendicular to the camera. This means that our appearance control method can also be applied to a non-Lambertian surface with a coaxial projector-camera system. In addition, we intend to make the system high-speed. As we mentioned in Limitations section, a projector-camera system with high-framerate devices can reduce the perception of flickering of projected area, and it can also be applied to environmental light that has temporal flickering. We expect that our system with a coaxial and high-speed implementation provides a much wider range of applications.

ACKNOWLEDGMENTS

This work was supported by JST ACT-I grant number JPMJPR17U1 and partially supported by JSPS KAKENHI grant number 16H04384.

REFERENCES

- [1] M. R. Mine, J. van Baar, A. Grundhöfer, D. Rose, and B. Yang, "Projection-based augmented reality in disney theme parks," *IEEE Comput.*, vol. 45, no. 7, pp. 32–40, Jul. 2012.
- [2] D. A. Basballe and K. Halskov, "Projections on museum exhibits: Engaging visitors in the museum setting," in *Proc. 22nd ACM Conf. Comput.-Human Interaction Special Interest Group Australia Comput.-Human Interaction*, 2010, pp. 80–87.
- [3] B. R. Jones, H. Benko, E. Ofek, and A. D. Wilson, "IllumiRoom: Peripheral projected illusions for interactive experiences," in *Proc. SIGCHI Conf. Human Factors Comput. Syst.*, 2013, pp. 869–878.

- [4] B. Jones, R. Sodhi, M. Murdock, R. Mehra, H. Benko, A. Wilson, E. Ofek, B. MacIntyre, N. Raghuvanshi, and L. Shapira, "RoomAlive: Magical experiences enabled by scalable, adaptive projector-camera units," in *Proc. 27th ACM Symp. User Interface Softw. Technol.*, 2014, pp. 637–644.
- [5] G. Yamamoto, T. Kuroda, D. Yoshitake, S. Hickey, J. Hyry, K. Chihara, and P. Pulli, "PiTaSu: Wearable interface for assisting senior citizens with memory problems," *Int. J. Disability Human Develop.*, vol. 10, no. 4, pp. 295–300, 2011.
- [6] T. Chen-Yoshikawa, E. Hatano, A. Yoshizawa, and H. Date, "Clinical application of projection mapping technology for surgical resection of lung metastasis," *Interactive Cardiovascular Thoracic Surg.*, vol. 25, pp. 1010–1011, 2017, doi:10.1093/icvts/ivx247.
- [7] R. Raskar, G. Welch, K.-L. Low, and D. Bandyopadhyay, "Shader lamps: Animating real objects with image-based illumination," in *Proc. 12th Eurograph. Workshop Rendering Techn.*, 2001, pp. 89–102.
- [8] A. H. Bermano, M. Billeter, D. Iwai, and A. Grundhöfer, "Makeup lamps: Live augmentation of human faces via projection," *Comput. Graph. Forum*, vol. 32, no. 2, pp. 311–323, 2017.
- [9] Y. Fujimoto, R. T. Smith, T. Taketomi, G. Yamamoto, J. Miyazaki, H. Kato, and B. H. Thomas, "Geometrically-correct projection-based texture mapping onto a deformable object," *IEEE Trans. Vis. Comput. Graph.*, vol. 20, no. 4, pp. 540–549, Apr. 2014.
- [10] G. Narita, Y. Watanabe, and M. Ishikawa, "Dynamic projection mapping onto a deformable object with occlusion based on high-speed tracking of dot marker array," in *Proc. 21st ACM Symp. Virtual Reality Softw. Technol.*, 2015, pp. 149–152.
- [11] T. Amano and H. Kato, "Appearance control using projection with model predictive control," in *Proc. 20th Int. Conf. Pattern Recognit.*, 2010, pp. 2832–2835.
- [12] S. K. Nayar, H. Peri, M. D. Grossberg, and P. N. Belhumeur, "A projection system with radiometric compensation for screen imperfections," in *Proc. ICCV Workshop Projector-Camera Syst.*, 2003.
- [13] M. D. Grossberg, H. Peri, S. K. Nayar, and P. N. Belhumeur, "Making one object look like another: Controlling appearance using a projector-camera system," in *Proc. IEEE Conf. Comput. Vis. Pattern Recognit.*, 2004, pp. 452–459.
- [14] A. Grundhöfer and O. Bimber, "Real-time adaptive radiometric compensation," *IEEE Trans. Vis. Comput. Graph.*, vol. 14, no. 1, pp. 97–108, Feb. 2008.
- [15] M. Brown, A. Majumder, and R. Yang, "Camera-based calibration techniques for seamless multiprojector displays," *IEEE Trans. Vis. Comput. Graph.*, vol. 11, no. 2, pp. 193–206, Mar./Apr. 2005.
- [16] K. Fujii, M. D. Grossberg, and S. K. Nayar, "A projector-camera system with real-time photometric adaptation for dynamic environments," in *Proc. IEEE Conf. Comput. Vis. Pattern Recognit.*, 2005, pp. 814–821.
- [17] J. Tsukamoto, D. Iwai, and K. Kashima, "Radiometric compensation for cooperative distributed multi-projection system through 2-DOF distributed control," *IEEE Trans. Vis. Comput. Graph.*, vol. 21, no. 11, pp. 1221–1229, Nov. 2015.
- [18] S. Mihara, D. Iwai, and K. Sato, "Artifact reduction in radiometric compensation of projector-camera systems for steep reflectance variations," *IEEE Trans. Circuits Syst. Video Technol.*, vol. 24, no. 9, pp. 1631–1638, Sep. 2014.
- [19] P. Pjanic, S. Willi, and A. Grundhöfer, "Geometric and photometric consistency in a mixed video and galvanoscopic scanning laser projection mapping system," *IEEE Trans. Vis. Comput. Graph.*, vol. 23, no. 11, pp. 2430–2439, Nov. 2017.
- [20] O. Bimber and D. Iwai, "Superimposing dynamic range," *ACM Trans. Graph.*, vol. 27, no. 5, 2008, Art. no. 150.
- [21] T. Amano and R. Suzuki, "Virtual recovery of the deteriorated art object based on AR technology," in *Proc. IEEE Conf. Comput. Vis. Pattern Recognit.*, 2007, pp. 1–2.
- [22] T. Amano and H. Kato, "Real world dynamic appearance enhancement with procam feedback," in *Proc. 5th ACM/IEEE Int. Workshop Projector Camera Syst.*, 2008, Art. no. 5.
- [23] O. Bimber, D. Klöck, T. Amano, A. Grundhöfer, and D. Kurz, "Closed-loop feedback illumination for optical inverse tone-mapping in light microscopy," *IEEE Trans. Vis. Comput. Graph.*, vol. 17, no. 6, pp. 857–870, Jun. 2011.
- [24] O. Bimber, A. Grundhöfer, D. Kurz, S. Thiele, F. Häntsch, T. Amano, and D. Klöck, "Projected light microscopy," in *Proc. ACM SIGGRAPH 2009: Talks*, 2009, Art. no. 69.
- [25] T. Amano and H. Kato, "Appearance control by projector camera feedback for visually impaired," in *Proc. Comput. Vis. Pattern Recognit. Workshop ProCams*, 2010, pp. 57–63.
- [26] M. Tanaka and T. Horiuchi, "Perception of gold materials by projecting a solid color on black materials," *Color Res. Appl.*, vol. 42, no. 4, pp. 522–530, 2016.
- [27] T. Amano, K. Komura, T. Sasabuchi, S. Nakano, and S. Yamashita, "Appearance control for human material perception manipulation," in *Proc. 21st Int. Conf. Pattern Recognit.*, 2012, pp. 13–16.
- [28] R. Akiyama, G. Yamamoto, T. Amano, T. Taketomi, C. Sandor, and H. Kato, "Appearance control in dynamic light environments with a projector-camera system," in *Proc. IEEE VR Workshop Perceptual Cogn. Issues AR*, 2016, pp. 1–6.
- [29] D. Cotting, M. Naef, M. Gross, and H. Fuchs, "Embedding imperceptible patterns into projected images for simultaneous acquisition and display," in *Proc. 3rd IEEE/ACM Int. Symp. Mixed Augmented Reality*, 2004, pp. 100–109.
- [30] A. Grundhöfer, M. Seeger, F. Häntsch, and O. Bimber, "Dynamic adaptation of projected imperceptible codes," in *Proc. 6th IEEE/ACM Int. Symp. Mixed Augmented Reality*, 2007, pp. 1–10.
- [31] R. Raskar, G. Welch, M. Cutts, A. Lake, L. Stesin, and H. Fuchs, "The office of the future: A unified approach to image-based modeling and spatially immersive displays," in *Proc. 25th Annu. Conf. Comput. Graph. Interactive Techn.*, 1998, pp. 179–188.
- [32] M. D. Fairchild, *Color Appearance Models*. Hoboken, NJ, USA: Wiley, 2013.
- [33] G. Yamamoto, L. Sampaio, T. Taketomi, C. Sandor, H. Kato, and T. Kuroda, "Imperceptible on-screen markers for mobile interaction on public large displays," *IEICE Trans. Inf. Syst.*, vol. 100, no. 9, pp. 2027–2036, 2017.
- [34] K. Sato, "Range imaging system utilizing nematic liquid crystal mask," in *Proc. 1st Int. Conf. Comput. Vis.*, 1987, pp. 657–661.
- [35] E. Mills and N. Borg, "Trends in recommended illuminance levels: An international comparison," *J. Illuminating Eng. Soc.*, vol. 28, no. 1, pp. 155–163, 1999.
- [36] K. Tajimi, K. Uemura, Y. Kajiwaru, N. Sakata, and S. Nishida, "Stabilization method for floor projection with a hip-mounted projector," in *Proc. 20th Int. Conf. Artif. Reality Telexistence*, 2010, pp. 77–83.
- [37] A. Dancu, Z. Franjic, and M. Fjeld, "Smart flashlight: Map navigation using a bike-mounted projector," in *Proc. 32nd Annu. ACM Conf. Human Factors Comput. Syst.*, 2014, pp. 3627–3630.
- [38] R. Akiyama, G. Yamamoto, T. Amano, T. Taketomi, A. Plopski, C. Sandor, and H. Kato, "Light projection-induced illusion for controlling object color," in *Proc. IEEE Conf. Virtual Reality 3D User Interfaces*, 2018, pp. 1–2.
- [39] D. Kelly, "Visual responses to time-dependent stimuli. I. Amplitude sensitivity measurements," *J. Opt. Soc. America*, vol. 51, no. 4, pp. 422–429, 1961.
- [40] A. Netravali, *Digital Pictures: Representation and Compression*. Berlin, Germany: Springer, 2013.
- [41] H. Park, B.-K. Seo, and J.-I. Park, "Subjective evaluation on visual perceptibility of embedding complementary patterns for nonintrusive projection-based augmented reality," *IEEE Trans. Circuits Syst. Video Technol.*, vol. 20, no. 5, pp. 687–696, May 2010.
- [42] J. Davis, Y.-H. Hsieh, and H.-C. Lee, "Humans perceive flicker artifacts at 500 Hz," *Sci. Rep.*, vol. 5, 2015, Art. no. 7861.
- [43] M. Ishikawa, "High-speed projector and its applications," in *Emerging Digital Micromirror Device Based Systems and Applications XI*. Bellingham, WA, USA: SPIE, 2019, Art. no. 109320N.
- [44] T. Amano, "Projection center calibration for a co-located projector camera system," in *Proc. IEEE Conf. Comput. Vis. Pattern Recognit. Workshops*, 2014, pp. 443–448.



Ryo Akiyama received the BE degree from Doshisha University, in 2015, and the ME degree from the Nara Institute of Science and Technology, in 2016. He is working toward the doctoral degree at the Nara Institute of Science and Technology. His research interests include augmented reality and projector-camera systems. He is a student member of the IEEE.



Goshiro Yamamoto received the BE, ME, and PhD degrees in engineering from Osaka University, Japan, in 2004, 2006, and 2009, respectively. Since 2016, he has been a senior lecturer with Kyoto University Hospital. His major research interests include human–computer interaction, projection-based augmented reality technologies, and wearable computing systems. He is a member of the IEEE.



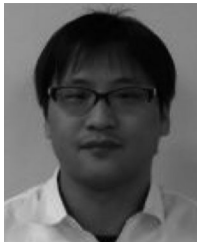
Alexander Plopski received the BSc and MSc degrees from the Technical University of Munich, in 2010 and 2012, respectively, and the PhD degree in information system design from Osaka University, in 2016. Since 2016, he has worked as an assistant professor with the Nara Institute of Science and Technology. He is a member of the IEEE.



Toshiyuki Amano received the PhD degree in engineering from Osaka University, Japan, in 2000. He is a professor with Wakayama University. Since 2012, he has been with Wakayama University. His research interests include spatial augmented reality, appearance manipulation, and installation art. He is a member of the IEEE.



Christian Sandor received the doctorate degree in computer science from the Munich University of Technology, Germany, in 2005 under the supervision of Prof. Gudrun Klinker and Prof. Steven Feiner. He is an associate professor with the City University of Hong Kong, where he is codirecting the Extended Reality Lab. He is a member of the IEEE.



Takafumi Taketomi received the BE degree from the National Institute for Academic Degrees and University Evaluation, in 2006, and the ME and PhD degrees in information science from the Nara Institute of Science and Technology, in 2008 and 2011, respectively. He works as an affiliate associate professor with the Nara Institute of Science and Technology. He is a member of the IEEE.



Hirokazu Kato received the BE, ME, and DrEng degrees from Osaka University, Japan, in 1986, 1988, and 1996, respectively. He is a professor with the Nara Institute of Science and Technology (NAIST), Japan. Since 2007, he has been with the Graduate School of Information Science of NAIST. He received the Virtual Reality Technical Achievement Award from IEEE VGTC, in 2009 and the Lasting Impact Award at the 11th IEEE International Symposium on Mixed and Augmented Reality, in 2012. He is a member of the IEEE.

▷ For more information on this or any other computing topic, please visit our Digital Library at www.computer.org/csdl.